

RESEARCH ARTICLE

Open Access



The chemical composition and manufacturing technology of glass beads excavated from the Hetian Bizili site, Xinjiang

Dong Wang^{1,2}, Rui Wen^{1,2*} , Julian Henderson³, Xingjun Hu⁴ and Wenyi Li⁴

Abstract

The Hetian Bizili site in Lop County, located on the southern route of the Silk Road in Xinjiang, China, was a trade and cultural hub between the East and the West in ancient times. In 2016, a large number of glass beads were unearthed from the 40 tombs excavated on this site. In this study we determined the chemical compositions and manufacturing technology of bodies and decorations of twelve glass beads from the M5 tomb of Bizili by using LA-ICP-AES, EDXRF, Raman Spectrometry, and SR- μ CT. The chemical compositions of the beads were all $\text{Na}_2\text{O}-\text{CaO}-\text{SiO}_2$, with plant ash mainly used as a flux. Lead antimonate and lead stannate were used as the opacifying agents. We detected elevated levels of boron and high levels of phosphorus in some beads: this is discussed in the context of the type of flux used and the possible use of a P-rich opacifier. Some of the beads with high contents of aluminum may potentially come from Pakistan. In terms of manufacturing technology, the craftsmen made 'eye' beads in different ways and also trail decorated beads.

Keywords: Glass eye beads, Xinjiang, The silk road, Bizili site

Introduction

The Xinjiang Uygur Autonomous Region, located in the northwest of China (Fig. 1), has been a vital area of cultural diversity and complexity [1]. Previously, archaeologists mainly focused on the Central Plains of China. Nowadays, Xinjiang has attracted more attention because the findings there can indicate the interactions among various populations as reflected in traded objects, technologies, and cultures [2]. A significant number of glass beads in various styles (including faience) have been excavated in the Xinjiang area during the past decades. Based on the published archaeological reports, the earliest faience in China, as early as 1900–1500 BC, was found at the Adunqiaolu site of Wenquan County, Xinjiang [3]. Moreover, a great number of faience beads have been unearthed at Tianshanbeilu (1500–1400 BC) and Ya'er

(1050–910 BC) in Hami [4, 5]. The earliest glass beads in China were found in Baicheng County and Tacheng County, Xinjiang, dating back to 1100–500 BC. They are all soda-lime glasses, believed to originate from the West. However, some of them have differences in their chemical compositions, which may conceivably be attributable to the use of local raw materials to make them [6]. Many glass beads spread to China carried by ancient nomadic people and all these sites are located in the north of Xinjiang far away from the Silk Road, indicating that cultural exchanges between the East and the West had started before the establishment of the Silk Road- or they may represent evidence for an early Silk Road. In comparison to the south of Xinjiang, the evidence of glass beads in this period is rare until the Han dynasty, when the evidence for them increased sharply. A large number of glass beads has been found in southern Xinjiang at Shampula [7], Niya [8, 9], Jierzankale [10] and Zhagunluke [11], with more than a thousand glass beads deriving from the former two sites which is more than is currently known from the area to the south of the Silk Road.

*Correspondence: rwen80@163.com

¹ Key Laboratory for Cultural Heritage Study & Conservation (Northwest University), Ministry of Education, Xi'an 710069, PR China
Full list of author information is available at the end of the article

Meanwhile, the number of glass beads in Northern Xinjiang is relatively small. Such a phenomenon may be linked to the influence of Zhang Qian in the Han dynasty. The Han government promoted trade and cultural exchanges between the Central Plains and Western regions. Also, those who travelled along the Silk Road including traders preferred the southern route because of safety concerns: the northeast of Xinjiang was occupied by the Huns.

The Bizili site is situated to the southeast of the Bizili Village, Lop County, in Southern Xinjiang (Fig. 1). The Xinjiang Institute of Cultural Relics and Archaeology excavated 40 tombs in cooperation with those constructing a road in 2016. According to the characteristics of these tombs, Bizili dates from the Han Dynasty (202 BC–220 AD) to the Wei and Jin Dynasties (220–420 AD). These tombs are all pit tombs and can be divided into convex-shaped pit tombs and rectangular pit tombs. M5 is the largest convex-shaped pit tomb and contains many bodies: ninety-seven human bones were found, with more females represented than males. Eleven more human bones were at the bottom of the tomb. Although the tomb was looted and burned sometime before it was excavated, a lot of finds were still preserved,

such as pottery, woodwork, pieces of iron, woolen fabrics, and beads. Notably, the first mutton-fat jade pendant to have been found in Xinjiang was discovered. The dry climate helped to preserve historic relics there [12].

In the Han dynasty (202 BC–220 AD), Bizili belonged to Khotan, a kingdom to the south of the Silk Road. This paper aims to investigate the technology used to make glass beads found there by using chemical analysis and to consider where the glass and the beads were made. It was hoped that this would provide useful evidence for the interaction, distribution, trade and exchange of glass beads along the terrestrial Silk Road as reflected in the beads found in the Bizili burials. We report some of the first trace element analysis of Chinese glasses.

Materials and methods

In this study, twelve glass beads excavated from tomb M5 at Bizili dating to the Western Han dynasty (202 BC–8 AD) were selected and chemically analysed. Table 1 provides a description of the samples, including the sizes and bead types. They all date to the Western Han Dynasty (202 BC to 8 AD). The majority of the samples were glass eye beads, a special type with an eye motif

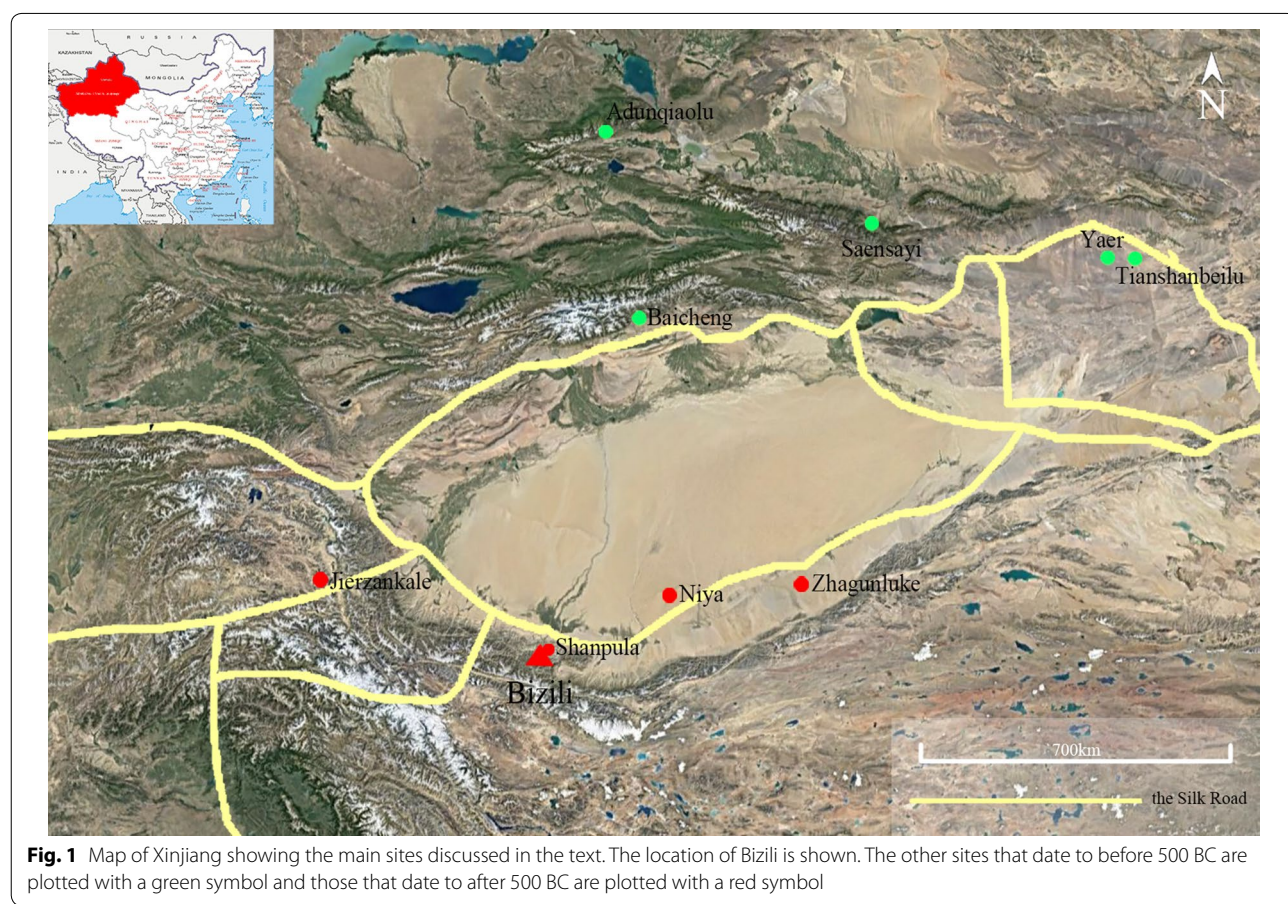
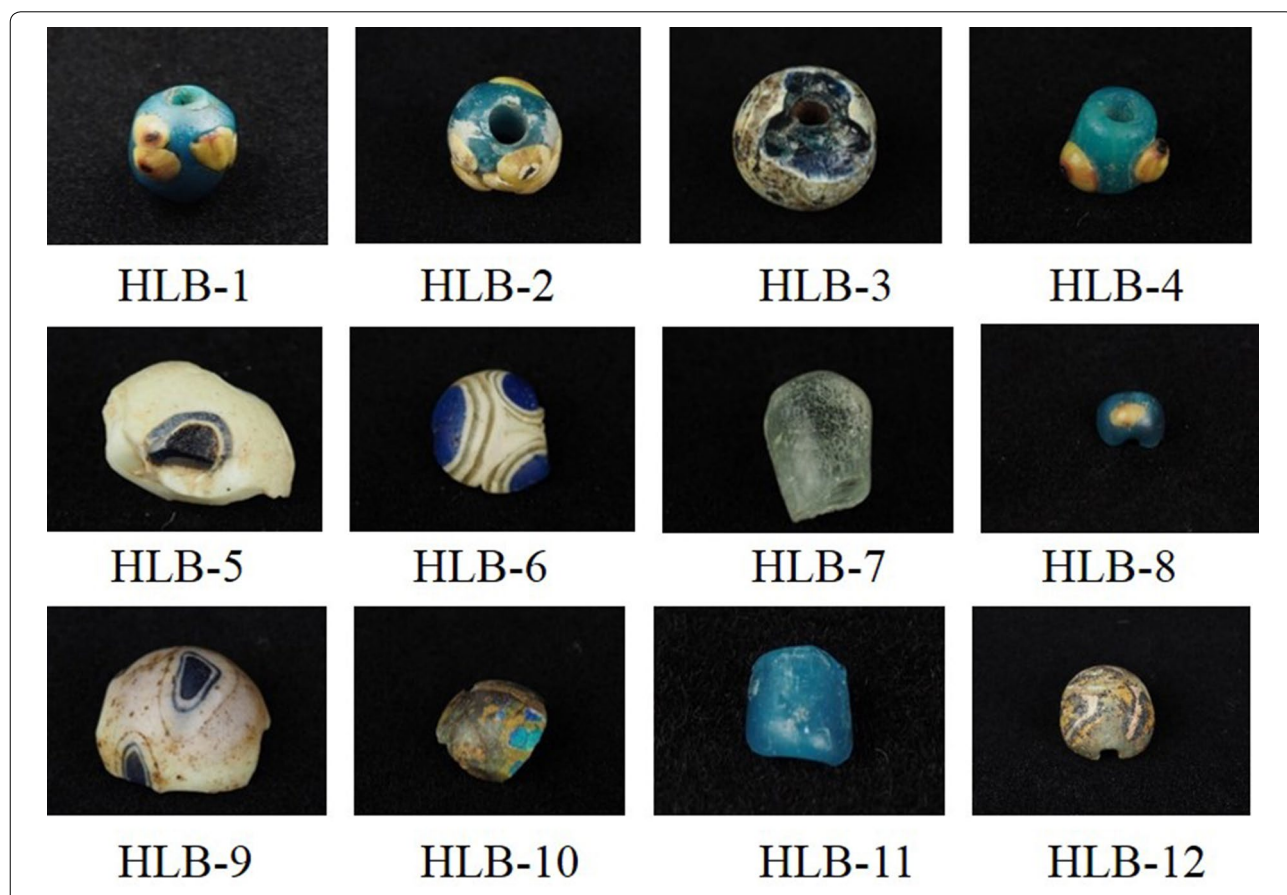


Table 1 Details of the glass beads from the Bizili site

| Sample | Size | Type |
|--------|--|-------------------------|
| HLB-1 | Diameter: 1 cm Aperture: 0.3–0.5 cm | Glass eye bead |
| HLB-2 | Diameter: 1.1 cm Aperture: 0.4 cm | Glass eye bead |
| HLB-3 | Diameter: 1.3 cm Aperture: 0.4 cm | Glass eye bead |
| HLB-4 | Diameter: 0.5 cm Aperture: 0.3 cm | Glass eye bead |
| HLB-5 | | Glass eye bead |
| HLB-6 | | Glass eye bead |
| HLB-7 | | Monochrome bead |
| HLB-8 | Diameter: 0.6 cm Aperture: 0.2 cm | Glass eye bead |
| HLB-9 | | Glass eye bead |
| HLB-10 | | Decorated glass bead |
| HLB-11 | Diameter: 0.35 cm Aperture: 0.2 cm | Monochrome bead |
| HLB-12 | Diameter: 1.4 cm Aperture: 0.35 cm | Glass bead with pigment |

set into monochrome bead surfaces [13]; only HLB 7 and HLB 11 are monochrome undecorated beads. Glass eye beads first appeared during the Eighteenth Dynasty of Egypt and was related to the ‘evil eye’ [14]. The Bizili glass beads were generally in good condition, some with different degrees of weathering on their surfaces. Photographs of all the beads are given in Fig. 2.

In this study, we observed beads using both optical microscopy and synchrotron radiation microtomography (SR- μ CT) to obtain technological information. The sample surfaces were cleaned using ethyl alcohol prior to examination. Optical microscopy observation was carried out in the School of Cultural Heritage, Northwest University. The instrument was a KH-7700 made by the HIROX Company, with a MX-5040RZF lens and a metal halogen cold light source. The sample was observed on at a 50 times magnification. SR- μ CT is a nondestructive 3D imaging technology that can reflect the internal structure of the objects and is suitable for archaeological study. The samples were scanned by synchrotron radiation micro X-ray fluorescence at the Shanghai Synchrotron Radiation Facility, Shanghai, China. The charge-coupled device detector has a spatial resolution of 5.2 μ m. The distance

**Fig. 2** The glass beads from Bizili, Xinjiang

between the detector and samples is 10 cm with the source energy of 28 keV.

Chemical compositions of the samples were determined using energy dispersion X-ray fluorescence spectrometry (ED-XRF) and laser ablation inductively-coupled plasma atomic emission spectroscopy (LA-ICP-AES). For the better preserved monochrome beads without complex ornaments, the bulk chemistry was determined using ED-XRF at the School of Cultural Heritage, Northwest University. The instrument used was a BRUKER ARTAX 400, fitted with a Mo anode. The primary X-ray beam used was 1 mm in diameter. The X-ray energy used was 30 kV, the current was 900 μ A, and the counting time was 300 s. During analysis, a helium purge was used to allow for the detection of light elements such as Na_2O and MgO . The standards used for calibration were Corning Glasses B, C and D. Table 2 shows the normalized major elemental contents of the glass standards compared with expected results. A total of 24 analyses are reported here (Table 4).

The beads decorated with complex patterns (HLB-1, HLB-2, HLB-3, HLB-4, HLB-5, HLB-6, HLB-8, HLB-9, HLB-10 and HLB-12) were analyzed using LA-ICP-AES to obtain quantitative chemical compositions of different parts of the glass beads. The analyses were performed in the School of Archaeology and Museology, Peking University. The LA-ICP-AES is equipped with a Nd-YAG laser and an RF generator of 40.82 MHz and 1.1 kw. The Q-switched laser mode was used with a laser wavelength of 266 nm and output energy of 10 ± 1 mJ. The auxiliary

gas pressure and nebulizer gas pressure were 0 psi and 30 psi, respectively. The Argon flow rate in the Plasma was 1.4 L/min. Helium was used as the carrier gas with a flow rate of 800 mL/min. Silica was used as an internal standard for minor and trace element analysis of the glass using this LA-ICP system. For major element analysis, external standards were used for calibration due to the different silica contents in samples and standards. The glass standards were Corning B and D from the Corning Museum of Glass. Table 3 shows the normalized major element contents of the glass standards.

Raman spectroscopy is a non-destructive method for analyzing the structure and the chemical bonds within the material by obtaining the characteristic wavelength frequencies of samples without special sample preparation. It was performed at the Emperor Qin Shihuang's Mausoleum Site Museum (Xi'an, Shaanxi) at room temperature, using a 514 nm Nd:YAG laser for the spectral range from 100 to 1000 cm^{-1} . A laser power of 10 mW was employed, and the acquisition time was 10 s for each integration which were accumulated 3 times. The attribution of the Raman signatures of crystalline phases was made by comparing them with data presented in the literature.

Results

Chemical composition

The chemical analyses of different glass colours for the 12 beads are given in Table 4, a total of 24 analyses. The very low levels especially of Na_2O are produced by weathering:

Table 2 Normalized major element contents of the glass standards (ED-XRF) (wt%)

| | Na_2O | MgO | Al_2O_3 | SiO_2 | P_2O_5 | K_2O | CaO | Fe_2O_3 | PbO |
|---------------------------|-----------------------|--------------|-------------------------|----------------|------------------------|----------------------|--------------|-------------------------|--------------|
| Corning B | | | | | | | | | |
| Average | 15.8 | 1.1 | 4.6 | 62.8 | 0.8 | 1.0 | 8.7 | 0.4 | 0.6 |
| RSD % | 14.0 | 63.0 | 10.0 | 1.0 | 8.0 | 4.0 | 2.0 | 7.0 | 4.0 |
| Reference composition wt% | 17.00 | 1.03 | 4.36 | 61.60 | 0.82 | 1.00 | 8.56 | 0.34 | 0.61 |
| Absolute error wt% | -1.20 | 0.07 | 0.24 | 1.20 | -0.02 | 0.00 | 0.14 | 0.06 | -0.01 |
| Relative error % | 7.06 | 6.80 | 5.50 | 1.95 | 2.44 | 0.00 | 1.64 | 17.65 | 1.64 |
| Corning C | | | | | | | | | |
| Average | 1.6 | 2.5 | 0.7 | 35.7 | 0.1 | 2.6 | 4.8 | 0.3 | 35.3 |
| RSD % | 58.0 | 60.0 | 50.0 | 4.0 | 19.0 | 15.0 | 10.0 | 14.0 | 6.0 |
| Reference composition wt% | 1.07 | 2.76 | 0.87 | 34.90 | 0.14 | 2.84 | 5.07 | 0.34 | 36.70 |
| Absolute error wt% | 0.49 | -0.29 | -0.13 | 0.81 | 0.01 | -0.21 | -0.28 | -0.03 | -1.39 |
| Relative error % | 45.36 | 10.69 | 14.90 | 2.33 | 4.29 | 7.51 | 5.61 | 7.55 | 3.79 |
| Corning D | | | | | | | | | |
| Average | 1.2 | 4.8 | 5.0 | 54.6 | 5.9 | 12.6 | 13.6 | 0.4 | 0.4 |
| RSD % | 91.8 | 11.2 | 2.8 | 1.8 | 3.5 | 1.6 | 1.1 | 1.5 | 1.3 |
| Reference composition wt% | 1.20 | 3.94 | 5.31 | 55.24 | 3.93 | 11.30 | 14.80 | 0.52 | 0.48 |
| Absolute error wt% | 0.0 | 0.9 | -0.3 | -0.6 | 2.0 | 1.3 | -1.2 | -0.1 | -0.1 |
| Relative error % | 0.00 | 21.83 | 5.84 | 1.16 | 50.13 | 11.50 | 8.11 | 23.08 | 16.67 |

Table 3 Normalized major element contents of the glass standards (LA-ICP-AES) (wt%)

| | Na ₂ O | MgO | Al ₂ O ₃ | SiO ₂ | P ₂ O ₅ | K ₂ O | CaO | Fe ₂ O ₃ |
|---------------------------|-------------------|------|--------------------------------|------------------|-------------------------------|------------------|-------|--------------------------------|
| Corning-d | | | | | | | | |
| Average | 1.38 | 3.99 | 5.73 | 53.98 | 4.05 | 12.41 | 15.24 | 0.55 |
| RSD % | 1.56 | 0.78 | 1.33 | 0.28 | 2.80 | 1.95 | 1.03 | 1.96 |
| Reference composition wt% | 1.20 | 3.94 | 5.31 | 55.24 | 3.93 | 11.30 | 14.80 | 0.52 |
| Absolute error wt% | 0.18 | 0.05 | 0.42 | -1.26 | 0.12 | 1.11 | 0.43 | 0.03 |
| Relative error % | 14.92 | 1.17 | 7.82 | 2.28 | 3.00 | 9.78 | 2.94 | 5.96 |
| Corning-b | | | | | | | | |
| Average | 16.14 | 1.06 | 4.61 | 62.68 | 0.90 | 0.95 | 9.01 | 0.39 |
| RSD % | 0.24 | 0.05 | 0.57 | 0.13 | 1.16 | 2.28 | 0.74 | 1.76 |
| Reference composition wt% | 17.00 | 1.03 | 4.36 | 61.60 | 0.82 | 1.00 | 8.56 | 0.34 |
| Absolute error wt% | -0.86 | 0.03 | 0.25 | 1.08 | 0.08 | -0.06 | 0.45 | 0.05 |
| Relative error % | 5.04 | 2.91 | 5.62 | 1.75 | 9.88 | 5.50 | 5.22 | 14.41 |

glass in the tomb can be weathered in variable ways, depending on microenvironments in the burial. In addition, the use of additives can lead to low Na₂O contents in glasses. The primary raw materials of glass are sands and fluxes often incorporating lime. Moreover, there will be deliberately added materials, such as chromophores and opacifiers and elements associated with them. These compounds would lead to a relatively low content of other components in glass. In this study, some samples (HLB6 white, HLB9 white, HLB10 green, HLB12 black, HLB12 white, HLB1yellow, HLB2yellow, HLB4yellow, HLB8yellow and HLB5white) have opacifiers. According to the research by Brill, we removed the additives, and recalculated the remaining oxides to bring their sum to 100%. The recalculated results show that the Na₂O levels increase [15, 16].

The rarity and fragility of cultural relics, such as glass beads, requires the use of non-destructive or minimally invasive analysis techniques. In our study, we used LA-ICP-AES to obtain the chemical compositions through multiple tests at different depths. Where possible, we chosen the best data for unweathered glass.

Based on their chemical compositions, all the glass beads from the Bizili site are of a soda-lime-silica composition but with variations in the relative concentrations of the alkaline fluxes present and lead oxide in coloured decoration. Soda concentrations in unweathered glasses range from 5.75 to 12.91%. Some glasses contain high potassium oxide levels of upto 7.1%, levels approximately equal to that of soda which can therefore be classified as mixed alkali glasses. Additionally, melting temperatures of opaque yellow glasses would have been reduced by the presence of upto 20% PbO.

Henderson and Warren [17], Shortland [18] and Duckworth et al. [19] noted that there is often an excess of

lead present in such opacified glasses to account for the amount needed to form lead-rich opacifying crystals, the excess lead being present in the glass matrix and therefore reducing the overall melting temperature of the glass [17–19].

The levels of calcium oxide in unweathered glasses varies from quite low (2.13%) to very high (15.99%). Beads HLB-1 blue, HLB2-blue and HLB10-green contain very high Al₂O₃ levels at 9.34%, 8.12% and 6.77% respectively. Very high P₂O₅ levels in four of the HBL-12 colours are unusual; the high levels in HLB2 and 9 should also be noted and will be discussed further below. Four of the opaque yellow components of the glass eye beads with turquoise blue bodies (HLB-1, HLB-2, HLB-4, and HLB-8) are similar in chemical compositions, except for some variation in the concentrations of SnO₂ and PbO in opaque yellow glasses. High antimony in white glasses is associated with a calcium antimonate opacifier (see below). Three out of four opaque white glasses (HLB5, HLB6 and HLB9) also contain PbO at between 5.4 and 7.11% so this would be dissolved in the glass matrices.

The similarity in chemical composition of these four beads includes some characteristics of the colorants: three contain between 0.61% CuO and 0.67% CuO; HLB1 contains 0.82% CuO. HLB1 and HLB2 contain 0.8 and 0.18% ZnO. This could indicate that scrap brass was used to colour them. However HLB1 and HLB2 also contain 0.44% SnO₂. Other turquoise beads are also coloured by CuO: HBL3, HBL9 appearing 'black' and HBL11; HBL8 contains 0.67% CuO but is weathered.

Two translucent glasses contain sufficient levels of CoO to colour them blue: the decoration of HLB5 appearing 'black' and the body of HLB6 but both are highly weathered. They are both further characterised by NiO and ZnO which it can tentatively be suggested are associated

Table 4 Major, minor and trace element oxide compositions of the glass beads (wt% oxide)

| Sample ID | SiO ₂ | Al ₂ O ₃ | Fe ₂ O ₃ | MgO | CaO | Na ₂ O | K ₂ O | Na ₂ O+K ₂ O | MnO | P ₂ O ₅ | TiO ₂ | Sb ₂ O ₃ | Method | Weathering degree |
|--------------|------------------|--------------------------------|--------------------------------|-------|------------------|-------------------|------------------|------------------------------------|-------------------------------|-------------------------------|------------------|--------------------------------|------------|-------------------|
| HLB1-blue | 46.14 | 9.34 | 3.20 | 2.34 | 15.99 | 7.76 | 6.50 | 14.26 | 0.29 | 4.16 | 0.61 | 0.15 | LA-ICP-AES | Unweathered |
| HLB1-yellow | 63.96 | 6.69 | 0.86 | 3.57 | 5.11 | 3.79 | 5.44 | 9.23 | 0.07 | 0.64 | 0.26 | 0.06 | LA-ICP-AES | Weathered |
| HLB2-blue | 66.40 | 8.12 | 1.86 | 2.65 | 6.27 | 3.76 | 4.97 | 8.73 | 0.15 | 2.93 | 0.52 | 0.06 | LA-ICP-AES | Weathered |
| HLB2-yellow | 52.33 | 4.89 | 1.03 | 1.69 | 4.23 | 2.48 | 3.36 | 5.84 | 0.05 | 2.85 | 0.28 | 0.07 | LA-ICP-AES | Weathered |
| HLB3-blue | 67.44 | 4.37 | 0.57 | 3.32 | 3.43 | 12.55 | 6.20 | 18.75 | 0.08 | 0.49 | 0.16 | 0.01 | LA-ICP-AES | Unweathered |
| HLB3-white1 | 72.54 | 4.81 | 1.77 | 2.39 | 7.51 | 2.29 | 5.30 | 7.59 | 0.32 | 0.29 | 0.36 | 1.35 | LA-ICP-AES | Weathered |
| HLB4-blue | 75.74 | 3.08 | 0.44 | 2.29 | 2.13 | 9.82 | 5.18 | 15 | 0.05 | 0.25 | 0.11 | 0.00 | LA-ICP-AES | Unweathered |
| HLB4-yellow | 66.89 | 4.82 | 0.50 | 3.05 | 3.43 | 8.57 | 7.11 | 15.68 | 0.14 | 0.40 | 0.18 | 0.01 | LA-ICP-AES | Unweathered |
| HLB5-black | 87.32 | 3.03 | 1.69 | 0.56 | 1.85 | 1.00 | 1.84 | 2.84 | 1.25 | 0.29 | 0.22 | 0.05 | LA-ICP-AES | Highly weathered |
| HLB5-white | 72.55 | 2.40 | 0.53 | 0.50 | 1.52 | 2.88 | 2.17 | 5.05 | 0.19 | 0.41 | 0.18 | 8.49 | LA-ICP-AES | Weathered |
| HLB6-blue | 87.32 | 2.65 | 1.03 | 0.76 | 2.54 | 1.75 | 1.98 | 3.73 | 0.36 | 0.34 | 0.24 | 0.09 | LA-ICP-AES | Highly weathered |
| HLB6-white | 70.20 | 2.40 | 0.48 | 0.74 | 2.55 | 5.75 | 2.75 | 8.5 | 0.76 | 0.35 | 0.14 | 8.15 | LA-ICP-AES | Unweathered |
| HLB7 | 91.72 | 1.27 | 0.74 | 0.88 | 2.70 | 0.16 | 1.45 | 1.61 | 0.07 | ND | 0.10 | 0.05 | ED-XRF | Highly weathered |
| HLB8-yellow | 67.60 | 4.60 | 1.06 | 2.52 | 2.83 | 8.64 | 5.95 | 14.59 | 0.13 | 0.36 | 0.19 | 0.00 | LA-ICP-AES | Unweathered |
| HLB8-blue | 83.84 | 6.69 | 0.48 | 1.70 | 1.84 | 1.00 | 2.71 | 3.71 | 0.09 | 0.29 | 0.21 | 0.01 | LA-ICP-AES | Highly weathered |
| HLB9-black | 72.34 | 6.86 | 0.74 | 0.42 | 2.15 | 3.05 | 5.45 | 8.5 | 0.22 | 2.93 | 0.69 | 0.59 | LA-ICP-AES | Weathered |
| HLB9-white1 | 74.27 | 2.55 | 0.37 | 0.55 | 3.57 | 5.94 | 2.30 | 8.24 | 0.73 | 0.26 | 0.12 | 3.40 | LA-ICP-AES | Unweathered |
| HLB10-green | 68.17 | 6.77 | 2.36 | 3.42 | 7.02 | 5.49 | 4.62 | 10.11 | 0.68 | 0.26 | 0.24 | 0.00 | LA-ICP-AES | Unweathered |
| HLB11-green | 81.24 | 4.31 | 1.30 | 1.71 | 4.23 | 0.49 | 2.80 | 3.29 | 0.22 | 0.02 | 0.27 | 0.28 | ED-XRF | Highly weathered |
| HLB12-blue | 66.32 | 4.99 | 0.48 | 4.06 | 3.38 | 12.91 | 6.05 | 18.96 | 0.08 | 0.39 | 0.16 | 0.00 | LA-ICP-AES | Unweathered |
| HLB12-black | 14.62 | 1.74 | 1.24 | 3.69 | 6.66 | 3.06 | 2.23 | 5.29 | 44.77 | 8.48 | 0.23 | 2.63 | LA-ICP-AES | unweathered |
| HLB12-pink | 54.56 | 4.16 | 2.97 | 12.11 | 5.54 | 2.08 | 5.22 | 7.3 | 0.40 | 8.02 | 0.48 | 0.08 | LA-ICP-AES | unweathered |
| HLB12-white1 | 44.02 | 3.01 | 1.87 | 2.43 | 6.40 | 2.64 | 2.69 | 5.33 | 5.38 | 7.69 | 0.27 | 1.55 | LA-ICP-AES | unweathered |
| HLB12-white2 | 20.50 | 2.11 | 1.41 | 2.97 | 10.20 | 2.40 | 2.71 | 5.11 | 9.26 | 17.18 | 0.52 | 1.73 | LA-ICP-AES | Unweathered |
| Sample ID | CuO | PbO | CoO | BaO | SnO ₂ | SrO | ZnO | B ₂ O ₃ | V ₂ O ₅ | NiO | ZrO | Ag ₂ O | Method | |
| HLB1-blue | 0.82 | 0.23 | 0.02 | 0.16 | 0.44 | 0.09 | 0.80 | 0.20 | 0.38 | 0.37 | 0.00 | 0.01 | LA-ICP-AES | Unweathered |
| HLB1-yellow | 0.08 | 7.02 | 0.00 | 0.15 | 1.86 | 0.05 | 0.15 | 0.09 | 0.07 | 0.06 | 0.01 | 0.00 | LA-ICP-AES | Weathered |
| HLB2-blue | 0.63 | 0.14 | 0.01 | 0.24 | 0.46 | 0.05 | 0.18 | 0.09 | 0.32 | 0.19 | 0.00 | 0.00 | LA-ICP-AES | Weathered |
| HLB2-yellow | 0.43 | 20.03 | 0.00 | 0.41 | 5.43 | 0.08 | 0.10 | 0.06 | 0.10 | 0.07 | 0.00 | 0.03 | LA-ICP-AES | Weathered |
| HLB3-blue | 1.03 | 0.00 | 0.00 | 0.09 | 0.04 | 0.05 | 0.01 | 0.10 | 0.02 | 0.04 | 0.00 | 0.00 | LA-ICP-AES | Unweathered |
| HLB3-white1 | 0.26 | 0.21 | 0.05 | 0.21 | 0.07 | 0.02 | 0.08 | 0.10 | 0.02 | 0.04 | 0.01 | 0.01 | LA-ICP-AES | Weathered |
| HLB4-blue | 0.61 | 0.00 | 0.00 | 0.14 | 0.02 | 0.03 | 0.00 | 0.05 | 0.01 | 0.02 | 0.00 | 0.00 | LA-ICP-AES | Unweathered |
| HLB4-yellow | 0.01 | 4.17 | 0.00 | 0.11 | 0.46 | 0.04 | 0.00 | 0.06 | 0.01 | 0.02 | 0.01 | 0.00 | LA-ICP-AES | Unweathered |
| HLB5-black | 0.16 | 0.00 | 0.09 | 0.13 | 0.11 | 0.03 | 0.07 | 0.14 | 0.05 | 0.11 | 0.00 | 0.00 | LA-ICP-AES | Highly weathered |
| HLB5-white | 0.08 | 7.11 | 0.00 | 0.01 | 0.40 | 0.01 | 0.12 | 0.21 | 0.08 | 0.16 | 0.00 | 0.00 | LA-ICP-AES | Weathered |
| HLB6-blue | 0.15 | 0.06 | 0.08 | 0.03 | 0.13 | 0.02 | 0.15 | 0.15 | 0.05 | 0.11 | 0.00 | 0.01 | LA-ICP-AES | Highly weathered |
| HLB6-white | 0.06 | 5.40 | 0.00 | 0.02 | 0.08 | 0.02 | 0.06 | 0.07 | 0.01 | 0.02 | 0.00 | 0.00 | LA-ICP-AES | Unweathered |
| HLB7 | 0.01 | 0.07 | 0.01 | 0.69 | 0.05 | 0.02 | 0.01 | ND | ND | ND | ND | ND | ED-XRF | Highly weathered |
| HLB8-yellow | 0.09 | 5.00 | 0.00 | 0.11 | 0.76 | 0.03 | 0.01 | 0.07 | 0.01 | 0.03 | 0.01 | 0.00 | LA-ICP-AES | Unweathered |
| HLB8-blue | 0.67 | 0.03 | 0.00 | 0.11 | 0.09 | 0.02 | 0.01 | 0.11 | 0.04 | 0.07 | 0.00 | 0.00 | LA-ICP-AES | Highly weathered |
| HLB9-black | 0.94 | 0.09 | 0.00 | 0.03 | 0.97 | 0.02 | 0.72 | 0.73 | 0.36 | 0.68 | 0.00 | 0.00 | LA-ICP-AES | Weathered |
| HLB9-white1 | 0.04 | 5.60 | 0.00 | 0.03 | 0.06 | 0.03 | 0.06 | 0.07 | 0.01 | 0.02 | 0.00 | 0.01 | LA-ICP-AES | Unweathered |
| HLB10-green | 0.09 | 0.00 | 0.00 | 0.16 | 0.19 | 0.05 | 0.02 | 0.11 | 0.19 | 0.16 | 0.00 | 0.01 | LA-ICP-AES | Unweathered |
| HLB11-green | 2.11 | 0.02 | 0.01 | 0.76 | 0.13 | 0.10 | 0.02 | ND | ND | ND | ND | ND | ED-XRF | Highly weathered |
| HLB12-blue | 0.88 | 0.00 | 0.00 | 0.08 | 0.02 | 0.06 | 0.00 | 0.08 | 0.01 | 0.02 | 0.01 | 0.00 | LA-ICP-AES | Unweathered |
| HLB12-black | 0.27 | 9.72 | 0.07 | 0.07 | 0.04 | 0.07 | 0.27 | 0.07 | 0.03 | 0.04 | 0.00 | 0.00 | LA-ICP-AES | Unweathered |
| HLB12-pink | 0.80 | 2.79 | 0.00 | 0.06 | 0.09 | 0.05 | 0.33 | 0.13 | 0.05 | 0.09 | 0.01 | 0.00 | LA-ICP-AES | Unweathered |
| HLB12-white1 | 0.10 | 21.46 | 0.01 | 0.05 | 0.07 | 0.08 | 0.16 | 0.07 | 0.02 | 0.03 | 0.00 | 0.00 | LA-ICP-AES | Unweathered |
| HLB12-white2 | 0.20 | 28.14 | 0.01 | 0.04 | 0.06 | 0.14 | 0.30 | 0.07 | 0.02 | 0.04 | 0.00 | 0.00 | LA-ICP-AES | Unweathered |

ND not detected

with the cobalt source. Moreover 0.09% CoO in the ‘black’ component of HLB12 may contribute to the colour—but 44.77% of MnO clearly dominates the colour. The analysis shows that it is mainly of the pigment on the bead’s surface.

Translucent blue and green glasses contain between 0.44 and 3.2% Fe₂O₃. Four contain MnO levels of below 0.09% so it would have been added adventitiously. The balance contains between 0.15 and 0.29% MnO. It is notable that the opaque yellow and white glasses also contain quite high levels of Fe₂O₃. The yellow glasses contain relatively low MnO, whereas opaque white glasses can contain up to 0.76% MnO (excluding HLB12).

Raman spectroscopy

As shown in Fig. 2, eight out of ten glass eye beads (HLB-1 to HLB-6, HLB-8, and HLB-9) are opaque or have opaque decoration. Raman spectroscopy was used to try to identify crystalline opacifiers in the glass without damaging the beads. Tests were conducted in the Emperor Qin Shihuang’s Mausoleum Site Museum only found peaks in HLB-4 and HLB-5 glass, possibly due to the weathering layers. Additional tests conducted at the Northwestern Polytechnic University gave same results. The results are shown in Figs. 3 and 4.

The results of Raman spectroscopy for the opaque yellow eyes show peaks at 134 cm⁻¹ and 322 cm⁻¹, similar to the peak for lead–tin yellow, a synthetic material that is widely used for making opaque yellow glass [20]. According to the crystalline structures and chemical compositions (Table 4), lead–tin yellow has two crystalline types, Pb₂SnO₄ and PbSn_{1-x}Si_xO₃. When compared to other published results [21], the opacifier used in the yellow eyes is PbSn_{1-x}Si_xO₃.

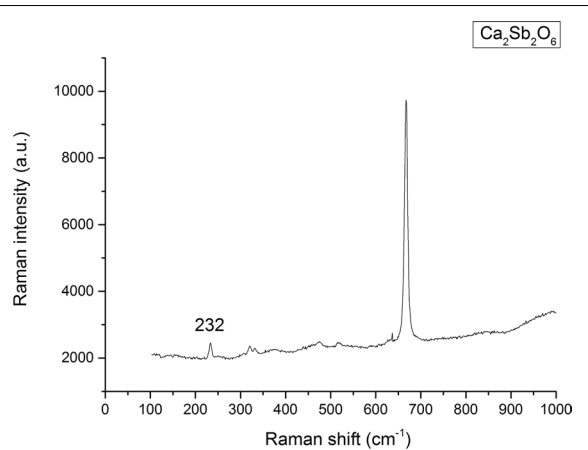


Fig. 4 Raman spectroscopic analysis of the opaque white body of bead HLB-5

Four beads among the opaque beads (HLB-3, HLB-5, HLB-6, and HLB-9) show high contents of antimony ranging from 1.35% to 8.49 wt% in the white parts; all were tested using Raman spectroscopy. Only the surface was analyzed to avoid damage to the sample. Only HLB-5 shows two peaks of different intensities at 232 cm⁻¹ and 667 cm⁻¹, corresponding to calcium antimonite (Ca₂Sb₂O₆) [13]. Other samples probably contain calcium antimonite used as an opacifier producing a white glass, but Raman didn’t produce results for them, probably because of weathering. Moreover, HLB12 has opaque white decoration which was found to contain high antimony. However, this also contains high P₂O₅ which will be discussed below.

Microscopic observation

Although the number of glass beads from Bizili is limited, they are rich in information about manufacturing processes. We found three special types of glass beads: eye beads, trail-decorated or possibly etched beads and beads with applied pigment decoration. Figures 5, 6, 7 show microscopic images of representative glass beads of different types. The optical microscope can reveal manufacturing traces on the surface of glass beads, while SR-μCT can reveal the internal structures.

The glass bead HLB-10 is fragmentary. The yellow decoration is probably trailed on but it is possible also that the surface was etched and the decoration inlaid. The possible evidence for etching is provided by observations under the microscope: see Fig. 6a. Figure 6b, c show the SR-Mct of the body and the decoration, respectively.

Discussion

Chemical compositions

As shown in Fig. 8, The plot of MgO versus K₂O in the glass beads shows two distinctive main groups. One has

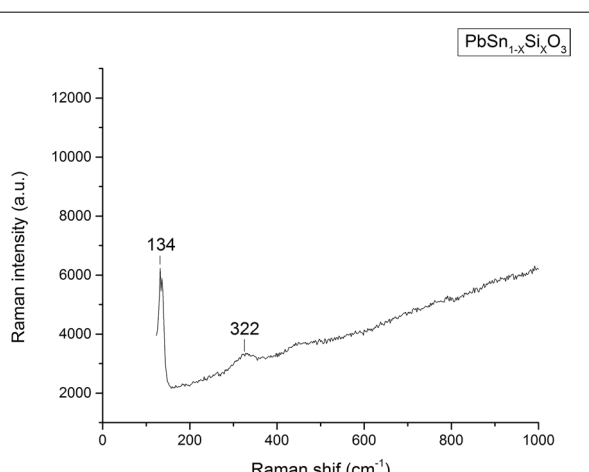


Fig. 3 Raman spectroscopic analysis of opaque yellow decoration of bead HLB-4

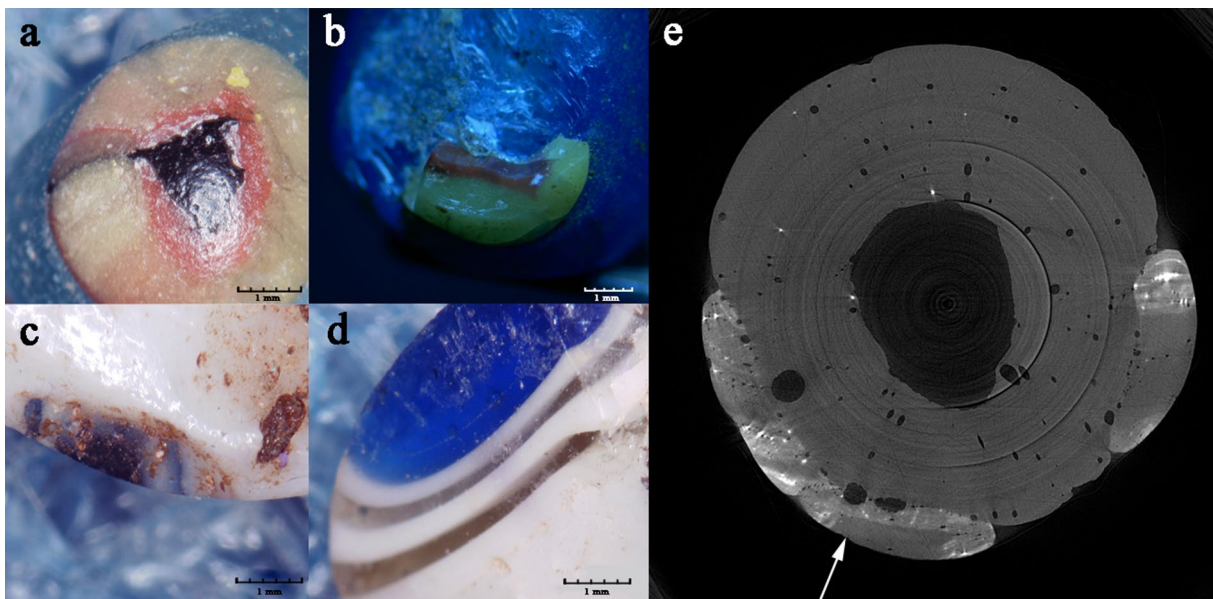


Fig. 5 Microscopic images of the glass eye beads (**a** HLB-1; **b** HLB-4; **c** HLB-9; **d** HLB-6; **e** HLB-1). **a-d** Show microscopic features of glass eyes in the beads. **e** Is the result of SR- μ CT showing the bead in section. The arrow indicates a location where one of the eyes is located on the bead

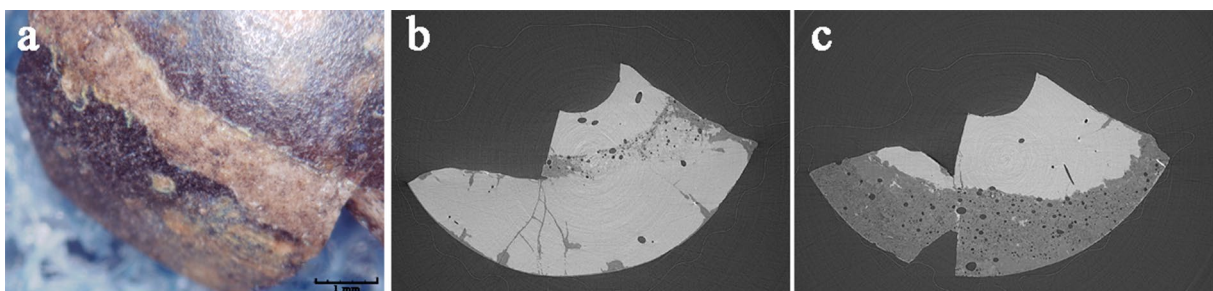


Fig. 6 Microscopic images of the glass bead with single stripe decoration (HLB-10)

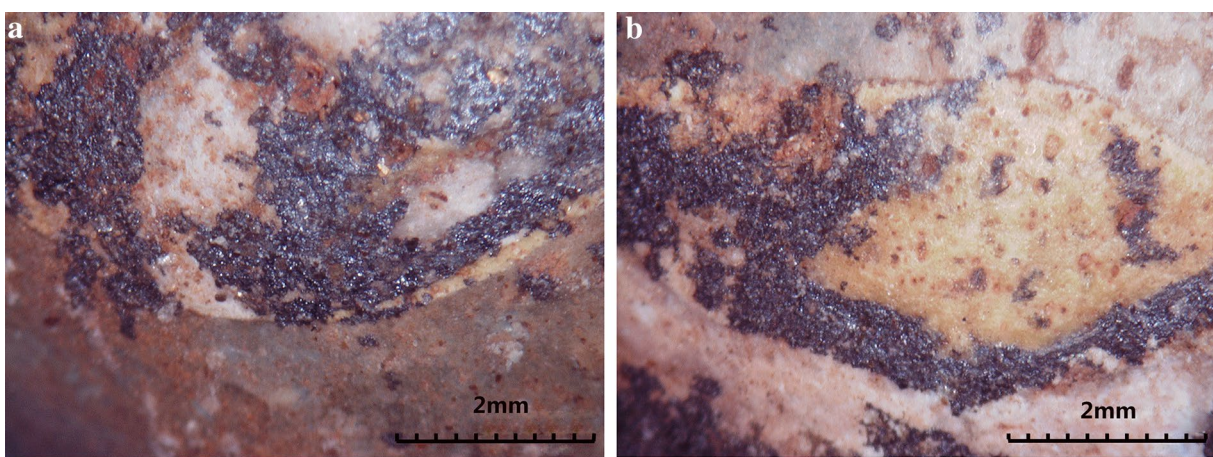


Fig. 7 Microscopic observation of glass bead HLB-12 showing opaque white decoration with black surface pigment

low magnesia and variable potassium oxide levels of up to 3%, the other contains c. 2–4% MgO and 4.5–7% K₂O. The first group consists of measurements of HLB-5, HLB-6, HLB-7 and HLB-9, including 2 measurements of different colours. There is a group of 3 glasses between the 2 main groups. One measurement (HLB9-black, with high Al₂O₃ (6.9%), 0.4% MgO and K₂O (5.5%) can be considered as an outlier. In Table 1 weathered and unweathered glasses are distinguished. Lower Na₂O and K₂O are often associated with the alkali being leached during weathering. The MgO and K₂O contents above 1.5 wt% indicate the use of a plant ash source of alkali. Those glasses with high potassium oxide and magnesia are therefore of a plant ash composition. Colorants used in the glasses are discussed above. The glasses that contain less than 1% MgO are nevertheless not natron glasses because they also contain elevated potassium oxide.

Natron glass is the predominant type of ancient glass in the Mediterranean and Europe from the around 1000 BC until the ninth century AD [22, 23]. However, the only 2 unweathered glasses with low magnesia levels, both opaque white glass in HBL6 and HBL9, contain higher potassium oxide levels than found in natron glasses (2.75 and 2.3% wt. oxide). Both contain low calcium oxide and high Sb₂O₃, because they are opacified with calcium antimonate, and 5.4/5.6% PbO. They have probably been made with a mineral source of alkali; the K₂O may have entered the glass as a potassium feldspar in the sands used. Other glasses containing low MgO are weathered and therefore do not warrant further discussion.

The second group beads (HLB-1, HLB-2, HLB-3, HLB-4, HLB-8, HLB-10, HLB-11, and HLB-12) had high total alkalies. All of them are characterized by high levels of both MgO and K₂O (over 1.5 wt%), suggesting that the

flux used was a plant ash. Plant ash can have quite variable chemical compositions according to the species of plants, the growing environment, the plant parts used, and the ashing temperatures [24]. Thus, the chemical compositions of the plant ash glass beads can vary from region to region too. The five plant ash glass beads from Bizili could derive from different regions. Five samples (HLB-1, HLB-2, HLB-4, HLB-8, and Hlb-10) are vegetal soda-lime glass (v-Na-Al glass) i.e. plant ash glass, with high Al₂O₃ of over 4%. They have MgO levels of between 1.7 and 3.5% and K₂O of between 2.7 and 7.1%. Dussubieux [25] identified three main types of v-Na-Al glass. The first type was found in Bara [26], north-east Pakistan, a site dating from the second century BC to the second century AD, which was the capital of the Kushan empire, though this does not mean the glasses were fused from raw materials there. They are mainly glass ornaments found in North India, China (Xinjiang) and Bangladesh. The other two types of v-Na-Al glass were found on sites dated to c. 900 AD and later so are not relevant to consider further here. Considering the spatial and temporal distribution of the v-Na-Al glass, our samples are closest in composition to those from Bara. The high contents of Al₂O₃ can be characteristic of central Asian glass; high alumina Indian glasses contain lower CaO. Four of the five glass beads are similar in appearance with blue bodies and yellow centres to the eyes with red and black concentric glass around the 'pupils'. This special type of glass eye beads is found in large quantities in Bara and named as the Bara-type beads [2, 9]. In terms of chemical compositions, the Bara beads are soda-based and characterized by relatively high Al₂O₃ and CaO levels varying from 4.4 to 9.4% [27]: these characteristics are similar to our samples although the blue matrix of HLB-1 has a mixed alkali composition. Collectively, the appearance, chemical compositions and distribution characteristics all suggest our glass beads may have originated from Bara. Though this does not prove that the glass used to make the beads was manufactured in Bara, it can nevertheless be suggested that the glasses used to make the beads were fused in Pakistan.

In addition to Bizili, the Bara-type glass beads have been found in many other sites in Xinjiang, including Shanpula [7], Niya [9] (shown in the Fig. 9) and Jierzankale [10]. Table 5 lists the details of the archaeological sites where Bara-type glass beads have been found in Xinjiang. Apart from Jierzankale, the other sites listed in Table 5 correspond to the date of Bara (second century BC to the second century AD). In addition to Bara, these other sites have produced bi-color glass beads with blue matrices and with and inlaid eyes with opaque yellow circles around their 'pupils' [28]. It is possible that the Bara-type glass eye beads from Shanpula, Niya and Bizili

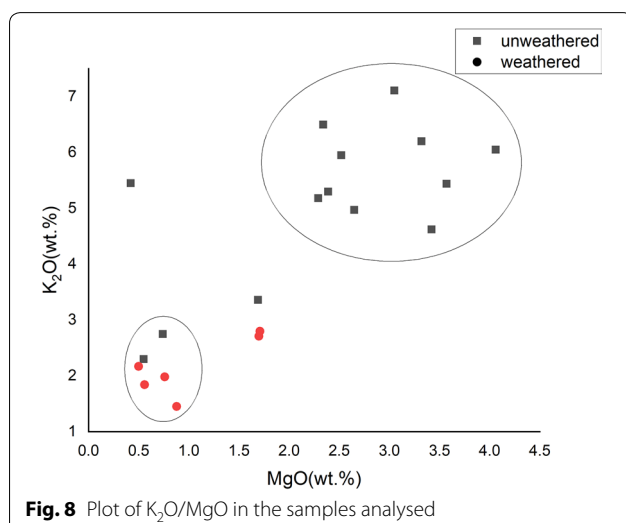


Fig. 8 Plot of K₂O/MgO in the samples analysed

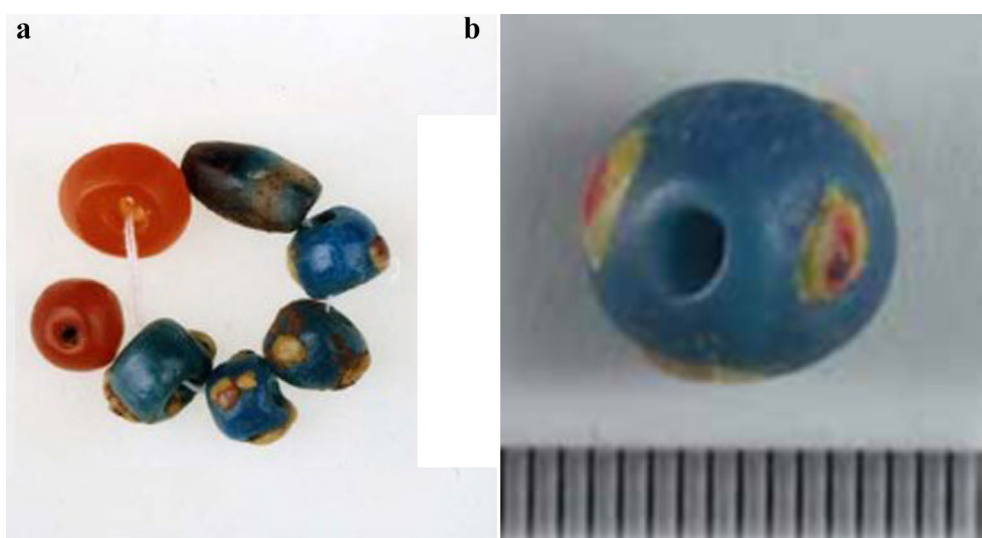


Fig. 9 Bara-type glass eye beads from other sites

Table 5 The information of the sites

| Site | Age |
|-------------|---------------|
| Jierzankale | 600–400 BC |
| Shanpula | 100 BC–400 AD |
| Niya | 202 BC–420 AD |
| Bizili | 202 BC–8 AD |

were made at Bara where evidence for glass working was found. However, without specific archaeological evidence for the production of these beads this must remain a tentative interpretation. The dating of Jierzankale (600–400 BC) is obviously earlier than that of Bara (and Bizili), showing that the glass beads found there with blue monochrome bodies decorated with multi-coloured could not have been made at Bara or other sites contemporary with Bara. It is possible that, if the eye beads from Bizili were made at Bara, their production was influenced by earlier bead making sites.

We undertook comparative studies of the published chemical compositions of contemporary glass from Mesopotamia, northern South Asia and Central Asia to investigate the possible origins of the Bizili glass beads. Some scholars consider that potash and alumina are very useful indicators in distinguishing plant ash glass from different origins [21]. With some exceptions, plant ash glass with K_2O higher than 4% can suggest a central Asian origin; plant ash glass from western Asia invariably contains less than 4%. From the research of Brill [15], a plot of Al_2O_3 versus K_2O shows distinctive groups of glass from Mesopotamia, Northern South Asia and

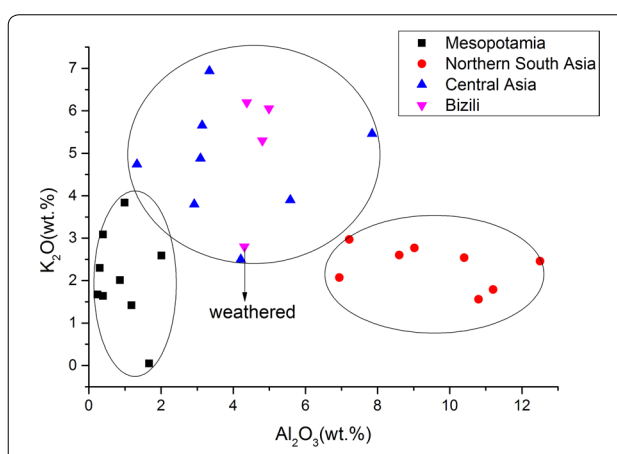


Fig. 10 Bi-plot of wt% K_2O versus wt% Al_2O_3 in glass beads from Bizili compared with contemporary glasses from sites in Mesopotamia, Northern South Asia and Central Asia

Central Asia. As shown in Fig. 10, Bizili results (for HLB-3, HLB-11 and HLB-12) fall into the Central Asian area of the plot, evidence that the glass used to make them probably originated from Central Asia. Many Bizili glasses contain elevated levels of boron. The highest level detected in unweathered glass is 2000 ppm in HLB1 blue; many other unweathered glasses contain c. 1000 ppm or below. Most are the plant ash glasses, some with high alumina and two contain low magnesia and elevated potassium oxide (HLB6 white and HLB9 white). The B is likely to have entered the plant ash glasses because the plants used were growing on boron-rich evaporitic soils, as originally suggested by Brill [29]. The alkali used in the

two examples of boron-rich glasses with low magnesium, both with 700 ppm B, may have been a borate mineral deposit, with the elevated K being introduced by K-rich minerals in the borate deposit; though the soda levels in these glasses appear low this is partly due to the presence of c. 5.5% PbO and 8.15 wt% and 3.4 wt% Sb₂O₃ respectively in the glasses. By deleting these additives the soda level would be raised.

Opacifiers

Ancient craftsmen obtained opaque glass by adding opacifying compounds to create a dispersion of crystals or heat treating the glasses to develop opacifying crystals out of the glassy matrix. These particles included tin oxide, lead–tin oxide, calcium antimonate and lead antimonate [30]. The opaque glass beads from the Bizili site has antimony-based and tin-based opacifiers, of which the former was used far earlier than the latter in ancient glass production.

Antimony-based opacifiers were used in Late Bronze Age Egypt and Mesopotamia from the mid-second millennium BC [18], in yellow lead-antimonate and white calcium antimonate. Tin based opacifiers were introduced from the second century BC and earlier [31–33], and from around the fourth century AD they tended to be the dominant opacifier used in glasses in the west [34].

The earliest lead stannate has been found in a glass bead from Sardis (the eighth to the seventh century BC) [33] and in glass beads from Poland [32].

Lead–tin oxide yellow glass became commoner in northwestern Europe at about the same time as white tin oxide glass, especially from the second century BC [30, 31] and was used by the Romans. During the early Islamic period (from about the eighth century AD), lead–tin oxide was commonly used [35, 36] and this continued as late as the Mamluk caliphate (thirteenth–fourteenth centuries) for the decoration of bottles and mosque lamps, for example.

Lead–tin yellow exists as Pb₂SnO₄ or PbSn_{1-x}Si_xO₃, both with high refractive indices (>2) [37]. During the production process of lead–tin yellow glass, the lead–tin calx, the fine powder that is left after heating a mixture of lead and tin to their melting points to temperatures above 600 °C is very important. The typical opaque yellow glass has a median Pb/Sn value of 9.1 [30]. In this study, except for HLB-4 with a Pb/Sn value of 9.07, the other three glass beads have relatively low Pb/Sn values (HLB-1 = 3.79; HLB-2 = 3.70; HLB-8 = 6.60).

The occurrence of high levels of P in Bizili glass beads is unusual. The blue matrix of HLB1 contains 4.16 wt% phosphorus pentoxide and the white decorative glass of HLB12 contains 17.18 wt% P₂O₅. Both of these glasses contain high calcium oxide levels too at 15.99% and

10.2% respectively. Other glasses mainly contain significantly lower levels of CaO so this suggests that bone ash may have been used to make the glass. Phosphorus pentoxide is invariably introduced into glasses when plant ash is used to make them [24], as is clear from our results. Tree ashes, and the glasses made from them, can contain higher levels of P₂O₅ [38, 39] but had they been used it is likely that much higher levels of e.g. MgO, K₂O, CaO and lower Na₂O (c. 2%) would have been detected in the Bizili glass beads. Therefore, a likely interpretation is that bone ash was used and that this is what has caused the very high levels of P and high Ca; it is possibly present as calcium phosphate [40] but this needs to be investigated further. Nevertheless, HLB12 black contains 8.02% P₂O₅ but much lower CaO, so this is less easy to interpret. This is comparable to the P₂O₅ levels in black beads reported by Liu et al. [2]. The use of bone ash in these beads appears to be the first time it has been detected in ancient central Asian glasses.

The use of opacifiers was not a common feature of glass-making in Ancient China, because antimony-based opacifiers and tin-based opacifiers were not found in lead-barium glass, potassium glass or high-lead glass made in China. There are a small number of exceptions such as two bluish-green high potassium glass beads from the Kizil cemetery (500–300 BC) which contained cassiterite and c. 6% tin oxide therefore probably opacified with tin oxide [41, 42]. First century AD white and yellow glasses from Guangxi Zhuang were also tin-opacified [43].

Thus, this supports the interpretation that the opaque glass beads from Bizili were imported. As the glass spread eastward, the use of opacifiers also gradually affected other areas. The kind of decoration used on Bara-type glass beads is likely to have been influenced by the West too.

Manufacturing technology of glass beads

The glass eye bead

The Bara-type glass eye beads and other glass eye beads show obvious differences. The Bara-type glass eye beads share similar appearances and chemical compositions but are of low quality. Eyes are not bonded closely to the body of the beads and often fall out (Fig. 5b). In comparison, other glass eye beads are well-made, and have stratified glass eyes which were prevalent in the Mediterranean from the 6th to third centuries BC, for example in Phoenician beads. Glass beads with a similar appearance dating to the fifteenth century BC have been found in Egypt [44] and also Mesopotamia later spreading to South Russia, Central Europe and other regions [45, 46]. During the East Zhou Dynasty (770–256 BC), glass production and the glass-making technique spread into

China. Compared with glass vessels, the technique of making a glass bead is simpler, so the early glass products in China are mainly glass beads. Available archaeological records show a large number of similar glass beads have been found in southern China [47]. These glass beads are mainly lead barium glass that is uniquely made in China. The development of China's early glass industry was likely influenced by the import of stratified eye glass beads. The craftsmen learned the glass bead manufacturing techniques and imitated the appearance of stratified eye glass beads with local raw materials.

The microscopic features of glass eye beads shown in Fig. 11 indicate two ways to make eyes for insertion in beads. In Fig. 11a, it is clear that the decoration is formed by a cut section from a rod with made from different colors. The manufacturers applied stratified glass saucers which appear as concentric circles on the surface by dropping liquid glass of different colors in sequence on top of each other (Fig. 11b) as shown by the traces in the flow lines in the glass. The other method used a glass rod produced by dipping into liquid glass of different colors in sequence to produce concentric circles of glass on a rod. When solidified, the rod was cut into sections of suitable sizes which were embedded into the base beads (Fig. 11a).

The variation of brightness on a CT slice reflects the differences in density and chemical composition, so the base glass of the beads and eyes can be clearly distinguished by different brightnesses. In general, air bubbles in glass are of standard spherical shapes during the vitrifying process [28]. In Fig. 5e, a lot of air bubbles of different shapes are dispersed through the base glass of the bead. Between the base glass and the eyes where the bubbles accumulated, they have an oblate shape and are bigger than elsewhere. This indicates that while the base glass was in a molten state, the craftsmen inserted the pre-made eyes into the beads. Between the beads and the eyes, the air bubbles were deformed by external pressure. As shown in Fig. 5e, the arrow indicates the direction of

pressure when eyes were inserted into the bead. Many small air bubbles fused to form a bigger bubble. This provides further evidence that the beads and eyes were made separately.

We drew a three-dimensional model based on the SR- μ CT data of sample HLB-1 as shown in Fig. 11 to show how the glass beads were made.

In general, ancient craftsmen mainly made glass beads by winding and drawing [48] normally, the bubbles in glass matrices were formed into standard spherical shapes during the vitrifying process but were deformed by winding and drawing [25]. The slender bubbles parallel to the perforation in Fig. 12b indicate that the glass bead was made by drawing. Ancient manufacturers used tools called a 'Lada,' a long hollow metal pipe, in conjunction with a mobile inner rod known as the chetak [49] to draw glass into glass tubes, and then cut them into glass beads. Slender elongated bubbles are the main feature of glass beads made by drawing. Figure 12c, d are enlargement of bubbles revealing more details. The shapes of bubbles in Fig. 12d is different from others with an ellipse at one end. In the glass bead making process, the shape of bubbles is changed a lot by pulling the glass.

The glass bead with single stripe decoration

As shown in Fig. 6, though the bead HLB-10 is fragmentary, the yellow band decorations could still be observed under the microscope. Figure 6a clearly shows the position of the decoration, while Fig. 6b, c show many differences between the body and decoration on the SR- μ CT. In Fig. 6b, a dense scatter of rounded gas bubbles can be seen. The consistent brightness reflects a uniform glass phase in terms of its chemical composition. Contrasting brightnesses can be seen in Fig. 6c. The inner part of the glass bead is brighter and has few bubbles, whereas the surface of the glass bead is darker and the structure is loose and porous with a large number of bubbles. The cause for this phenomenon is likely related to the manufacturing technology

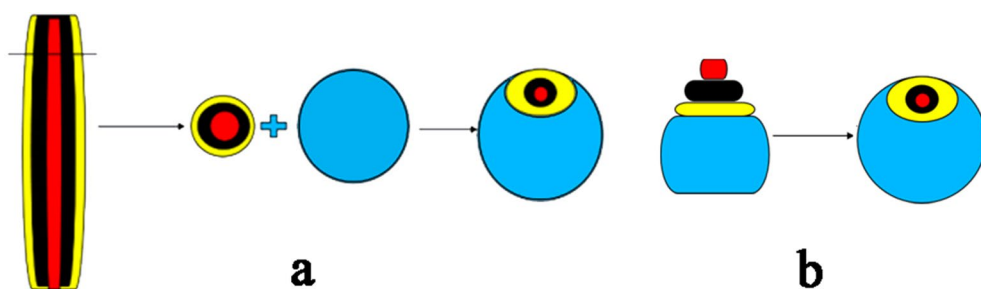
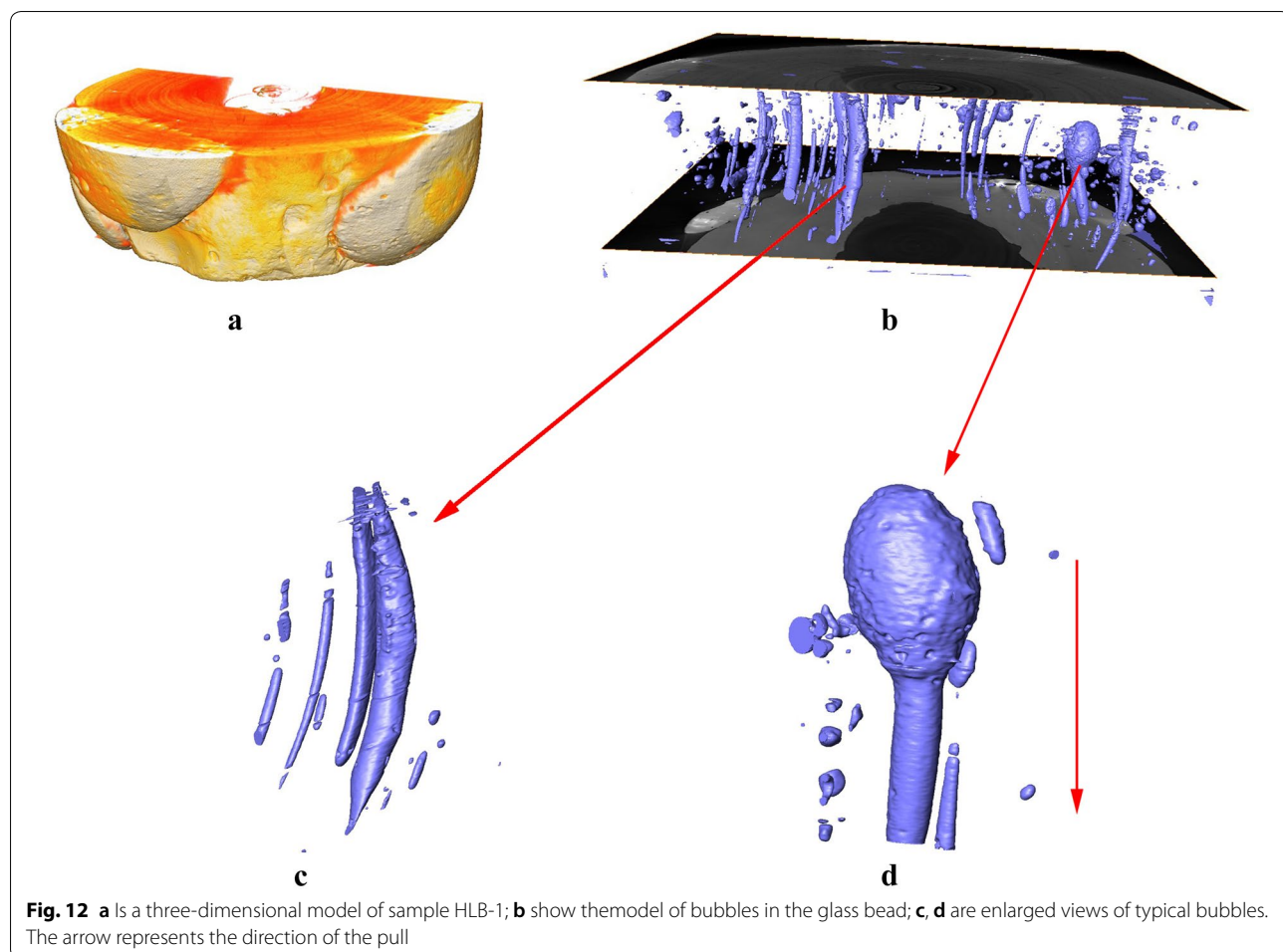


Fig. 11 The manufacturing process of stratified glass eye beads (HLB-1, HLB-2, HLB-4, HLB-8). **a** The method of making glass eye bead in dropping glass liquid; **b** the method of making glass eye bead in cutting off rods



that may have been used as used for etched carnelian beads, though an alternative decorative technique is trail decorating. Early etched carnelian beads were found at the Chanhudaro site of the Harappa Culture in the Indus Valley at first. If etching was used the craftsmen firstly mixed a special plant juice with alkali, then etched out patterns on the body of the bead, and buried the beads in charcoal ash for permanent decoration. A large number of etched carnelian beads have been excavated in India and they display a range of decorative patterns, including a cruciform ornament [50]. By using SR- μ CT we are suggesting one possible decorative technique is etching. This could explain why in the area of the decoration there are a lot of bubbles because of chemical reactions between glass and alkali. The alkali solution penetrates downward, producing a corrosion layer. Therefore we are suggesting that this is a new type of glass bead decoration influenced by the etched carnelian beads, although trail decoration cannot be excluded.

The glass bead with pigment

The glass beads with pigment (HLB-12) has a blue base with eye-like decorations. According to the results of LA-ICP-AES, the base glass is a central Asian plant ash soda-lime glass as discussed above, coloured with 0.88% CuO. The black pigment contains low SiO₂ and high MnO₂ (44.7%) so perhaps pyrolusite, a manganese-rich mineral, was mixed with a ground glass to produce a black pigment. The white area contains 21.4–28.1% of PbO, but also 44% SiO₂, low total alkali, 5.38% MnO, 7.69% P₂O₅ and 1.35% Sb₂O₃ indicating that the material used was possibly a combination of ground glass, mineral pigments and bone ash. Optically the pigment layer appears very thin, of less than one millimeter thickness with a lot of particles. In the process of making glass beads, the craftsmen fused the monochromatic glass to make the base bead and then applied different ornamentation on the bead surface with pigments of different colors. To combine the base bead and the pigments, these glass beads were probably fired

again. When the temperature is high, the decoration could become less regular due to the fluidity of glass.

The glass beads with pigment are rarely found in archaeological excavations except in China. Based on archaeological reports [14, 51], using pigments to decorate glass beads already appeared in the Central Plains area of China during the Warring States period. The chemical composition of the matrix of HLB-12 corresponds to a Central Asian origin, suggesting such decorative methods probably developed in Central Asia in the Western Han dynasty. However, given that the technology appeared earlier in China than in Central Asia, we don't exclude the possibility that Central Asia was influenced by China.

Conclusion

The occurrence of early glass in China mainly occurred near the Tianshan Mountains in Xinjiang, and was related to links with Mesopotamia and Europe. After the Western Han Dynasty, the occurrence of glass along the south of the Silk Road grew explosively, and the impact of India had become manifest [52, 53]. This study has analyzed glass beads from Bizili located on the southern part of the terrestrial Silk Road. They are mostly $\text{Na}_2\text{O}-\text{CaO}-\text{SiO}_2$, and were made with plant ash as fluxes including a smaller number of possible borate glasses. A comparative study of the chemical compositions and appearances of glass beads from other regions shows that the Bizili beads have strong foreign cultural characteristics and are believed to have originated from Central Asian and possibly from the Kushan area, including Bara in Pakistan which was a capital of the Kushan Empire.

Among the samples, there are four glass beads (blue monochrome base glasses decorated with multi-coloured eyes) which are very similar to beads from Bara. These special type of glass eye beads were found in large number in Bara, but it doesn't mean that they were created there, nor does it mean that the glasses used to make the beads were made in or near Bara. The latest archaeological evidence shows that this kind of glass bead had appeared before the Bara site, such as at Jierzankale [10]. Therefore, the Bizili beads may possibly have been made earlier than the date of Bizili and/or their production was influenced by other production in areas of central Asia, depending on how many sites specialised in making them. In addition, some opaque glass beads were opacified with antimony-based and tin-based opacifiers. Moreover, it appears that calcium phosphate was present in the beads and may have been used as an opacifier.

In terms of glass bead making technology, there are two ways to make eyes for glass eye beads of the Bara type; the beads themselves were made by drawing. Meanwhile, 2 new types of glass bead decoration were discovered including a possible etched type and a glass bead decorated with pigments.

This research suggests that Bizili was influenced by many cultures, especially central and southern Asia. With the development of the Silk Roads, the trade and the cultural exchange between various regions became more frequent, leading to the appearance of glass objects in large quantities during the Han dynasty.

Abbreviations

SR- μ CT: Synchrotron radiation microtomography; ED-XRF: Energy dispersion X-ray fluorescence spectrometry; LA-ICP-AES: Laser ablation inductively-coupled plasma atomic emission spectroscopy.

Acknowledgements

This study was sponsored by the National Natural Science Foundation of China (Grant No. 11575142), 111 project (D18004) and the students' innovation and entrepreneurship training program of school of cultural heritage, Northwest University (2019WYYCY-04). Special thanks go to the Shanghai Synchrotron Radiation Facility for helping with the analysis and the Xinjiang Institute of Cultural Relics and Archaeology for providing the glass beads samples in this study. Thanks to Jianfeng Cui for debugging instrument and calibration of LA-ICP-AES. Many thanks also to Xiaoya Zhan for modifying the language.

Authors' contributions

DW and RW designed the research described in this paper. All the experiment was done by DW. DW and RW drafted the majority of the manuscript. JH edited and modified the paper. XH and WL provided the samples in this study. All authors read and approved the final manuscript.

Funding

Beyond the National Natural Science Foundation of China (Grant No. 11575142) support, the 111 project (D18004) and the students' innovation and entrepreneurship training program of school of cultural heritage, Northwest University also supported this research (2019WYYCY-04).

Availability of data and materials

Please contact the corresponding author for reasonable data requests.

Ethics approval and consent to participate

This article does not contain any studies with human participants or animals performed by any of the authors.

Consent for publication

The consent for the publication of details and images in the manuscript are obtained from all participants.

Competing interests

The authors declare that they have no competing interests.

Author details

¹ Key Laboratory for Cultural Heritage Study & Conservation (Northwest University), Ministry of Education, Xi'an 710069, PR China. ² Research Center for Archaeological Science, Northwest University, Xi'an 710069, PR China.

³ Department of Classics and Archaeology, University of Nottingham, University Park, Nottingham NG7 2RD, UK. ⁴ Xinjiang Institute of Cultural Relics and Archaeology, Urumchi 830000, PR China.

Received: 26 March 2020 Accepted: 25 November 2020

Published online: 08 December 2020

References

- Chen G. Study on the cultures of the Bronze Age and early Iron Age in Xinjiang area. *Archaeology*. 1990;4:366–74 (**In Chinese**).
- Liu S, Li QH, Gan F, Zhang P, Lankton JW. Silk Road glass in Xinjiang, China: chemical compositional analysis and interpretation using a high-resolution portable XRF spectrometer. *J Archaeol Sci*. 2012;39(7):2128–42.

3. Yingzhu W. The technological research of faience in Western Zhou and Eastern Zhou periods. University of science and technology Beijing, Doctoral dissertation. 2019. p. 1–6 (**In Chinese**).
4. Liu N, Yang Y, Wang Y, et al. Nondestructive characterization of ancient faience beads unearthed from Ya'er cemetery in Xinjiang, Early Iron Age China. *Ceram Int*. 2017;43(13):10460–7.
5. Xinjiang Institute of Cultural Relics and Archaeology. Saensiay site of Xinjiang, China. *Cultural Relics*. 2013. p. 1–261 (**In Chinese**).
6. Gan F, Li Q, Gu D, et al. Study on early glass beads unearthed from Baicheng and Tacheng of Xinjiang. *J Chin Ceram Soc*. 2003;07:663–8.
7. Xinjiang Institute of Cultural Relics and Archaeology. Shapula, Xinjiang, China. The Peoples Press of Xinjiang. 2001. p. 1–239 (**In Chinese**).
8. Yu Z. Archaeological excavation of Niya site M8 cemetery in Xinjiang. *Cult Relics*. 2000;2000(1):4–40 (**In Chinese**).
9. Lin Y. A scientific study of glass finds from the Niya site in Xinjiang, Doctoral dissertation. 2009. p. 1–171 (**In Chinese**).
10. Wu X. Archaeological excavation of Jierzankale Cemetery in Xinjiang in 2013. *West Reg Stud*. 2014;2014(1):124–7 (**In Chinese**).
11. Cheng Q, Guo JL, et al. Characteristics of chemical composition of glass finds from the Qiemo tombsites on the Silk Road. *Spectrosc Spectr Anal*. 2012;32(7):1955–60.
12. Hu X, et al. New archaeological discovery of Bizili Cemetery in Luopu County, Xinjiang. *West Reg Stud*. 2017;2017(1):144–6 (**In Chinese**).
13. Yang J, Zhao HX, Yu P. Analysis of composite glass beads (eye-beads) unearthed from the Shahe Tomb in the Changping District of Beijing. *Sci Conserv Archaeol*. 2012;24(2):74–83 (**In Chinese**).
14. Zhao D. Exotic beads and pendants in ancient China: from western Zhou to eastern Jin Dynasty. Beijing: Science Press; 2016. p. 54–5 (**In Chinese**).
15. Brill R. (with a contribution by Brandt A. Rising). Chemical analyses of early glasses. Corning: The Corning Museum of Glass; 1999.
16. Panighello S, Ortega EF, Elteren JTV, et al. Analysis of polychrome Iron Age glass vessels from Mediterranean I, II and III groups by LA-ICP-MS. *J Archaeol Sci*. 2012;39(9):2945–55.
17. Henderson J, Warren SE. X-ray fluorescence of Iron Age glass: beads from Meare and Glastonbury Lake Villages. *Archaeometry*. 2010;23(1):83–94.
18. Shortland A. The used and origin of antimonate colorants in early Egyptian glass. *Archaeometry*. 2002;44(4):517–30.
19. Duckworth C, Henderson J, Rutten FJM, Nikita K. Opacifiers in late Bronze Age glasses: the use of ToF-SIMS to identify raw ingredients and production techniques. *J Archaeol Sci*. 2012;39:2143–52.
20. Cheng Q, Guo J. The use of antimony and tin in ancient western glass making. In: Tenth national symposium on archaeology and heritage conservation. 2008. p. 386–92 (**In Chinese**).
21. Liu S. The development of portable X-ray fluorescence analysis and its application in scientific and technological archaeology, Doctoral dissertation. 2011. p. 77–95 (**In Chinese**).
22. Sayre EV, Smith RV. Compositional categories of ancient glass. *Science*. 1961;133(3467):1824–6.
23. Gallo F, Silvestri A, Molin G. Glass from the archaeological museum of Adria (North-East Italy): new insights into Early Roman production technologies. *J Archaeol Sci*. 2013;40(6):2589–605.
24. Barkoudah Y, Henderson J. Plant ashes from Syria and the manufacture of ancient glass: ethnographic and scientific aspects. *J Glass Stud*. 2006;48(1):297–321.
25. Dussubieux L, Gratuze B, Blet-Lemarquand M. Mineral soda alumina glass: occurrence and meaning. *J Archaeol Sci*. 2010;37(7):1646–55.
26. Dussubieux L, Gratuze B. Nature et origine des objets en verre retrouvés à Begram (Afghanistan) et à Bara (Pakistan). In: Bopearachchi O, Landes C, Sachs C, editors. *De l'Indus à l'Oxus: Archéologie de l'Asie Centrale*. Lattes: Association Imago, Musée de Lattes. 2003. p. 315–23.
27. Dussubieux L, Gratuze B. Glass in South Asia. In: Janssens K, editor. *Modern methods of analyzing archaeological and historical glass*. New York: Wiley; 2013. p. 401–30.
28. Cheng Q, Zhang X, Guo J, et al. Application of computed tomography in the analysis of glass beads unearthed in Shapula cemetery (Khotan), Xinjiang Uyghur Autonomous Region. *Archaeol Anthropol Sci*. 2019;11:937–45.
29. Brill RH, Stapleton CP. Chemical analyses of early glasses, vol. 3, The years 2000–2011, Reports and Essays. Corning Museum of Glass, Corning, New York. 2012.
30. Matin M. Tin-based opacifiers in archaeological glass and ceramic glazes: a review and new perspectives. *Archaeol Anthropol Sci*. 2018;11(4):1–13.
31. Henderson J. The raw materials of early glass production. *Oxf J Archaeol*. 1985;4(3):267–91.
32. Purowski T, Dzierżanowski P, Bulska E, Wagner B, Nowak A. A study of glass beads from the Hallstatt C-D from southwestern Poland: implications for glass technology and provenance. *Archaeometry*. 2012;54:144–66.
33. Van Ham-Meert A, Dillis S, et al. A unique recipe for glass beads at Iron Age Sardis. *J Archaeol Sci*. 2019;108:0305–4403.
34. Biek L, Bayley J. Glass and other vitreous materials. *World Archaeol*. 1979;11:1–25.
35. Fiorentino S, Vandini M, Chinni T, Caccia M, Martini M, Galli A. Colourants and opacifiers of mosaic glass tesserae from Khirbet al-Mafjar (Jericho, Palestine): addressing technological issues by a multi-analytical approach and evaluating the potentialities of thermo-luminescence and optically stimulated luminescence dating. *J Archaeol Anthropol*. 2017;11:1–23.
36. Fiorentino S, Chinni T, Cirelli E, Arletti R, Conte S, Vandini M. Considering the effects of the Byzantine-Islamic transition: Umayyad glass tesserae and vessels from the qasr of Khirbet al-Mafjar (Jericho, Palestine). *J Archaeol Anthropol*. 2018;10:223–45.
37. Clark RH, Cridland L, Kariuki BM, Harris KDM, Withnall R. Synthesis, structural characterization and Raman spectroscopy of the inorganic pigments lead-tin yellow types I and II and lead antimonate yellow: their identification on medieval paintings and manuscripts. *J Chem Soc Dalton Trans*. 1995;16:2577–82.
38. Jackson CM, Booth CA, Smedley JW. Glass by design? Raw materials, recipes and compositional data. *Archaeometry*. 2005;47:781–95.
39. Meek A, Henderson J, Evans J. The isotopic analysis of English Forest glass from the Weald and Staffordshire. *J Anal Atomic Spectrosc*. 2012;27:786–95.
40. Silvestri A, Nestola F, Peruzzo L. Multi-methodological characterisation of calcium phosphate in late-antique glass mosaic tesserae. *Microchem J*. 2016;124:811–8.
41. Li QI, Liu S, Zhao HX, Gan FX. Characterization of some ancient glass beads unearthed from the Kizil reservoir and Wanquan cemeteries in Xinjiang, China. *Archaeometry*. 2014;56:601–24.
42. Henderson J, An J, Ma H. The archaeology and archaeometry of Chinese glass: a review. *Archaeometry*. 2018;60:88–104.
43. Zhao HX, Li QH, Liu S, Gan FX. Characterisation of microcrystals in some ancient glass beads from China by means of confocal Raman microscopy. *J Raman Spectrosc*. 2013;44:643–9.
44. Gan F. Development of Chinese ancient glass. Shanghai: Shanghai Scientific & Technical Publishers; 2016. p. 69–75 (**In Chinese**).
45. Spaer M. Some observations on the stratified Mediterranean eye-beads of the first millennium BC. *Association internationale pour l'histoire du verre. Annales du 10e congrès de l'association internationale pour l'histoire du verre 1985*. Amsterdam: International Association for the History of Glass; 1987. p. 1–12.
46. Spaer M. Ancient glass in the Israel museum beads and other small objects. Jerusalem: The Israel Museum; 2001.
47. Yu Y. Research on beads unearthed from Hunan Province. Changsha: Hunan People's Publishing House; 2018. p. 50–253 (**In Chinese**).
48. Jiayao A. A brief history of glasswares in China. Beijing: Social Sciences Academic Press; 2011. p. 49–51 (**In Chinese**).
49. Kanungo AK. Glass beads in Indian archaeology: an ethnoarchaeological approach. *Bull Deccan Coll*. 2001;60–61:337–53.
50. Zhao D. Study on etched carnelian beads unearthed in China. *Archaeology*. 2011;10:68–78 (**In Chinese**).
51. Huang X, Yan J, Wang H. Analysis of the decorated silicate beads excavated from Tomb M4 of the Ma-Jia-Yuan Warring States Cemetery, Gansu Province. *Spectrosc Spectr Anal*. 2015;35(10):2895–900 (**In Chinese**).
52. Cheng Q, Chun Yu, Xi L, He W. A test and preliminary study of the composition of the glass excavated from the Norbutso Site of Ngari in Tibet and a discussion of the Silk Road in Ngari. *J Tibetol*. 2017;02:264–74 (**In Chinese**).
53. Lv H. The study on the early burials in the western Himalaya region. *Acta Archaeol Sin*. 2015;2015(1):1–34 (**In Chinese**).

Publisher's Note

Springer Nature remains neutral with regard to jurisdictional claims in published maps and institutional affiliations.